

This is the accepted manuscript made available via CHORUS. The article has been published as:

# Chemotaxis Driven Instability of a Confined Bacterial Suspension

T. V. Kasyap and Donald L. Koch

Phys. Rev. Lett. **108**, 038101 — Published 18 January 2012

DOI: [10.1103/PhysRevLett.108.038101](https://doi.org/10.1103/PhysRevLett.108.038101)

# Chemotaxis driven instability of a confined bacterial suspension

T. V. Kasyap and Donald L. Koch

*School of Chemical and Biomolecular Engineering, Cornell University, Ithaca, New York 14853*

A suspension of bacteria in a thin channel or film subject to a gradient in the concentration of a chemoattractant, will develop, in the absence of an imposed fluid flow, a steady bacteria concentration field that depends exponentially on cross-stream position. Above a critical bacteria concentration, this quiescent base state is unstable to a steady convective motion driven by the active stresses induced by the bacteria's swimming. Unlike previously identified long wavelength instabilities of active fluids, this instability results from coupling of the bacteria concentration field with the disturbance flow.

PACS numbers: 87.17.Jj, 87.18.Hf, 47.57.E-, 47.63.Gd

Observations that suspensions of swimming bacteria with no imposed stresses or chemical gradients exhibit collective motions on length scales large compared with an individual cell have inspired simulations of hydrodynamically interacting Stokesian swimmers and continuum theories for bacteria suspensions [1]. The continuum theories feature an active stress resulting from the force dipoles the cells exert as they swim. The homogeneous, quiescent state of an unbounded suspension governed by these equations has been shown to be unstable to perturbations in bacteria orientation distribution that couple with the fluid shearing induced by the active stresses [1–4]. Since the purpose of bacterial motility is to allow cells to respond to chemical cues in their environment, it is of interest to explore how bacterial collective motion may be altered by chemical gradients. In this Letter, we show that bacteria suspensions exhibit a new type of instability (illustrated in Fig. 1) when the cells' swimming motion is biased due to a gradient of a chemical attractant in a confined channel or liquid film. The new instability involves coupling of active stress induced fluid convection with the bacteria concentration field.

Two recent experimental studies suggest that bacteria do exhibit enhanced convection in the presence of chemoattractant gradients. Kim and Breuer [5] observed a significant increase in the hydrodynamically induced diffusivity of a fluorescent molecule in a suspension of wild type *E. Coli* as the concentration gradient of an attractant was increased. Sokolov *et al.* [6] studied the dynamics of thin films of aqueous suspensions of aerobic *B. Subtilis* cells. As they increased the thickness of these films, they observed a transition from spatially homogeneous, coherent motion in the plane of the film to a strongly convective, spatially inhomogeneous three dimensional motion. The onset of convective motion coincided with the development of cross-film gradients of oxygen, which acts as an attractant for the cells. While gravitational forces due to cell concentration variations can lead to “bio-convection” [7], the film thickness and associated Rayleigh number in Sokolov *et al.*'s experiment [6] was too small to admit such an instability. We suggest instead that the motion was induced by an instability

associated with the active stress of chemotactic bacteria.

While chemical attractants are often consumed or produced by bacteria, the simplest setting in which to explore chemical effects on the motion of a bacteria suspension is that illustrated in Fig. 1, where a linear gradient is imposed across a channel of thickness  $H$  in the  $z$  direction and infinite extent in the  $x$  direction with no slip walls. Cheng *et al.* [8] have designed an apparatus where a linear gradient of an attractant, such as Me-Asp ( $\alpha$ -methyl-DL-aspartate) that is not consumed by bacteria [9] and has a diffusivity large compared with that of the cells, can be established by the attractant diffusing across a sealed micro-channel sandwiched between source and sink channels.

In the absence of velocity and chemical gradients, bacteria such as *E. Coli* or *B. Subtilis* perform an unbiased random walk comprised of intervals of persistent swimming lasting about  $\tau_0 \approx 1$ s punctuated by short intervals of ‘tumbling’ [10]. The state of a dilute bacterial suspension can be specified by the singlet probability den-

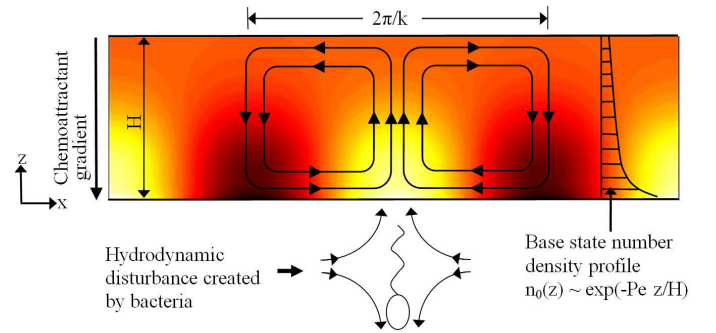


FIG. 1. Mechanism of the chemotaxis driven instability. Individual bacteria align in the direction of the chemical gradient leading to dipolar fluid velocity disturbances. At the continuum level, the instability manifests itself through the perturbed number density field represented by color contours and the streamline pattern illustrated within the channel. Brighter regions indicate higher bacteria concentrations. The fluid motion acting on the base state number density profile sweeps bacteria toward the region of high perturbed bacteria concentration leading to growth of the perturbation.

sity  $\Omega(\mathbf{x}, \mathbf{p}, t)$  where  $\mathbf{p}$  and  $\mathbf{x}$  are the orientation and the position of a bacterium [1, 3, 4].  $\Omega(\mathbf{x}, \mathbf{p}, t)$  satisfies a Boltzmann-like equation with the tumbling of the bacterium being modelled as a Markov process [4]. On length scales much larger than the persistence length  $U\tau_0$  where  $U$  is the swimming speed of the bacteria,  $\Omega(\mathbf{x}, \mathbf{p}, t)$  can be decomposed into a number density field  $n(\mathbf{x}, t)$  and an orientation field  $f(\mathbf{p}, t)$ . In the absence of fluid flow, the steady-state orientation distribution  $f(\mathbf{p})$  can be obtained by equating the rate  $f(\mathbf{p})/\tau$  at which cells tumble away from orientations near  $\mathbf{p}$  with the rate at which cells tumble into the region near  $\mathbf{p}$ . Assuming for simplicity that pre- and post-tumble orientations are uncorrelated, the latter rate is  $\frac{1}{4\pi} \int f(\mathbf{p})/\tau d\mathbf{p}$  [4]. In presence of a chemoattractant gradient, the bacteria bias their random walk by reducing  $\tau^{-1}$  when moving up the gradient and leaving it unaltered when swimming down the gradient [10], so that  $\tau^{-1}$  has been described by [11]:

$$\tau^{-1} = \begin{cases} \tau_0^{-1} \exp(-\zeta \mathbf{p} \cdot \mathbf{g}) & \text{if } \mathbf{p} \cdot \mathbf{g} > 0, \\ \tau_0^{-1} & \text{if } \mathbf{p} \cdot \mathbf{g} \leq 0, \end{cases} \quad (1)$$

where  $\mathbf{g} = -\mathbf{e}_z$  is the unit vector parallel to the chemical gradient,  $\zeta = \chi U G$ ,  $G$  is the magnitude of the gradient, and  $\chi$  is the sensitivity of bacteria to the attractant. Using the linearized form of Eq. (1) for weak chemotaxis,  $\zeta \ll 1$ , the orientation field obtained by equating the rates of direct and inverse events [12] is

$$f(\mathbf{p}) = \begin{cases} \frac{1}{4\pi} [1 + (\mathbf{p} \cdot \mathbf{g} - 1/4)\zeta] + O(\zeta^2) & \text{if } \mathbf{p} \cdot \mathbf{g} > 0, \\ \frac{1}{4\pi} [1 - \zeta/4] + O(\zeta^2) & \text{if } \mathbf{p} \cdot \mathbf{g} \leq 0, \end{cases} \quad (2)$$

The resulting mean orientation  $\langle \mathbf{p} \rangle = (1/6)\zeta \mathbf{g}$  leads to a mean bacterial velocity  $\mathbf{U}_0 = U \langle \mathbf{p} \rangle$  parallel to the chemoattractant gradient. Typically, the magnitude of chemotactic drift velocity  $U_0 = |\mathbf{U}_0|$  is about 10% of the swimming speed [13], so that the theory with weak chemotaxis ( $\zeta \ll 1$ ) will be reasonably accurate. On time and length scales larger than  $\tau_0$  and  $U\tau_0$ , the number density satisfies a conservation equation with a chemotactic convective flux and a diffusive flux with the diffusivity  $D = U^2\tau_0/3$  arising from the unbiased part of the run-and-tumble motion [14]:

$$\frac{\partial n}{\partial t} + \nabla \cdot [(\mathbf{U}_0 + \mathbf{u})n - D\nabla n] = 0. \quad (3)$$

The fluid velocity  $\mathbf{u}(\mathbf{x}, t)$  and pressure  $p(\mathbf{x}, t)$  fields satisfy Stokes equations [1–4]

$$\begin{aligned} \nabla \cdot \mathbf{u} &= 0, \\ -\nabla p + \mu \nabla^2 \mathbf{u} + \nabla \cdot \sigma^B &= 0, \end{aligned} \quad (4)$$

where the bacterial stress is given by  $\sigma^B = -C\mu UL^2 \int \Omega [\mathbf{p}\mathbf{p} - \frac{1}{3}\mathbf{I}] d\mathbf{p}$ . Here  $\mu$  is the viscosity of the suspending fluid,  $L$  is the combined length of the bacterial cell and propulsive flagellar bundle, and  $C$  is

the force-dipole a bacterium exerts non-dimensionalized by  $\mu UL^2$ .  $C$  is positive for swimmers whose propulsive mechanisms push the cells and negative for pullers. The common bacterial species *E. Coli* and *B. Subtilis* are pushers with  $C = 0.57$  [4]. The anisotropic orientation distribution in Eq. (2) leads to an anisotropic bacterial stress tensor  $\sigma^B(\mathbf{x}, t) = n(\mathbf{x}, t)\mathbf{S}$  where the stresslet  $\mathbf{S} = -(C/16)\mu UL^2\zeta [\mathbf{g}\mathbf{g} - \frac{1}{3}\mathbf{I}]$ . Being a pusher, the bacterium exerts a pressure in the  $z$  direction (negative normal stress) and tension (positive normal stress) in the  $x$  and  $y$  directions. Although the orientation field in Eq. (2) changes after the onset of the instability due to rotation of bacteria by fluid velocity gradients, one can model the effects of this change on the bacterial stress in terms of a modified viscosity for disturbances with wavelengths larger than  $(nL^2)^{-1}$  [4, 12]. This viscosity is nearly isotropic when  $\zeta \ll 1$  [12]. Since the effects of such a modified viscosity on the stability of the suspension have been analyzed previously, we focus instead on the active normal stress difference induced directly by the chemical gradient. In addition, we neglect the  $O(\zeta^2)$  change in  $\mathbf{U}_0$  due to shear induced cell rotation.

Eqs. (3), (4), and (5) admit a stationary base state solution with no fluid flow and an exponential number density profile  $n_0(z) = \frac{\langle n_0 \rangle Pe \exp(-Pe z/H)}{1 - \exp(-Pe)}$  determined by the balance of cross-channel chemotaxis and diffusion. Here the angle brackets indicate an average over the channel cross-section and  $Pe = U_0 H/D = 3(\frac{H}{U\tau_0})(U_0/U)$  is a Peclet number measuring the strength of the chemotactic drift. In the base state, the inhomogeneous bacterial stress is balanced by the base state pressure  $p_0 = S_{zz}n_0$ .

We will now study the stability of this stationary base state to small perturbations of the bacteria number density and pressure fields, i.e.,  $n = n_0(z) + n'(x, z, t)$  and  $p = p_0(z) + p'(x, z, t)$  with  $n' \ll n_0$  and  $p' \ll p_0$  and fluid velocity perturbations  $\mathbf{u}'(x, z, t)$ . We adopt a lubrication approximation in which the variations with respect to  $x$  occur over a wavelength  $\lambda$  which is much larger than the channel thickness  $H$ , i.e.,  $\epsilon = H/\lambda \ll 1$ . Non-dimensionalizing  $z$  with the channel thickness  $H$ ,  $x$  with wavelength  $\lambda$ ,  $n$  with the gap averaged number density  $\langle n_0 \rangle$ ,  $p$  with the bacterial stress  $-\frac{3}{2}S_{zz}\langle n_0 \rangle$ ,  $u_x$  with  $U_0\epsilon$  and  $u_z$  with  $U_0\epsilon^2$  yields the following linearized lubrication equations. The  $x$ -momentum equation involves a balance between the viscous stress, the pressure gradient and the gradient of the bacterial stress:

$$-\beta \frac{\partial p'}{\partial x} + \frac{\beta}{3} \frac{\partial n'}{\partial x} + \frac{\partial^2 u'_x}{\partial z^2} = 0, \quad (6)$$

where  $\beta = -\frac{3S_{zz}\langle n_0 \rangle H}{2\mu U_0} = \frac{3}{8}C\langle n_0 \rangle L^2 H$  is a non-dimensional gap-averaged bacterial concentration that reflects the relative strength of the bacterial and viscous stresses.

The  $z$  momentum equation is a balance of the pressure

gradient and bacterial stress gradient

$$\frac{\partial p'}{\partial z} + \frac{2}{3} \frac{\partial n'}{\partial z} = 0, \quad (7)$$

which integrates to  $p'(x, z, t) = -\frac{2}{3}n'(x, z, t) + \bar{p}(x, t)$  where  $\bar{p}(x, t)$  is a  $z$  independent pressure field that assures that there is no net fluid flux in the  $x$  direction. The bacteria number density equation is:

$$\frac{\partial^2 n'}{\partial z^2} + Pe \frac{\partial n'}{\partial z} + \epsilon^2 \left[ \frac{\partial^2 n'}{\partial x^2} - \frac{\partial n'}{\partial t} - Pe u'_z \frac{\partial n_0}{\partial z} \right] = 0. \quad (8)$$

In the above equations, time has been non-dimensionalized by  $\epsilon^{-2}H^2/D$  so that the unsteady term  $\frac{\partial n'}{\partial t}$  balances the fluid convective term. It will be seen that this coupling term is the origin of the instability. The dominant balance in the bacteria conservation equation between chemotaxis and diffusion in the  $z$  direction yields a quasi-steady, local perturbed number density profile that is similar to the base state profile

$$n'(x, z, t) = \langle n' \rangle(x, t) \frac{Pe \exp(-Pe z)}{1 - \exp(-Pe)}, \quad (9)$$

The gap-averaged number density  $\langle n' \rangle(x, t)$  will be determined from the  $O(\epsilon^2)$  gap-averaged bacteria conservation equation. The solution of the  $x$  momentum equation with no slip boundary conditions is

$$u'_x = \beta \left\{ \left[ \frac{1 - \exp(-Pe z)}{Pe[1 - \exp(-Pe)]} - \frac{z}{Pe} \right] \frac{\partial \langle n' \rangle}{\partial x} + \frac{1}{2} \frac{\partial \bar{p}}{\partial x} (z^2 - z) \right\} \quad (10)$$

where the pressure gradient determined by the constraint of no net fluid flux ( $\langle u'_x \rangle = 0$ ) is

$$\frac{\partial \bar{p}}{\partial x} = 6 \frac{Pe[1 + \exp(-Pe)] + 2[\exp(-Pe) - 1]}{Pe^2[1 - \exp(-Pe)]} \frac{\partial \langle n' \rangle}{\partial x}. \quad (11)$$

Integrating Eq. (8) over  $z = (0, 1)$  and using the no-flux and no-slip boundary conditions yields the gap averaged bacteria concentration equation:

$$\frac{\partial \langle n' \rangle}{\partial t} + Pe \frac{\partial \langle u'_x n_0 \rangle}{\partial x} - \frac{\partial^2 \langle n' \rangle}{\partial x^2} = 0, \quad (12)$$

which shows that the gap-averaged concentration perturbation evolves due to the fluid convective and run-and-tumble diffusive fluxes in the  $x$  direction. The convective flux will be proportional to  $\frac{\partial \langle n' \rangle}{\partial x}$  with a sign dependent on whether the swimmers are pushers or pullers. Using the fluid velocity field in Eq. (10) driven by bacterial stresses to evaluate the convective flux, Eq. (12) takes the form:

$$\frac{\partial \langle n' \rangle}{\partial t} + (Pe\alpha\beta - 1) \frac{\partial^2 \langle n' \rangle}{\partial x^2} = 0, \quad (13)$$

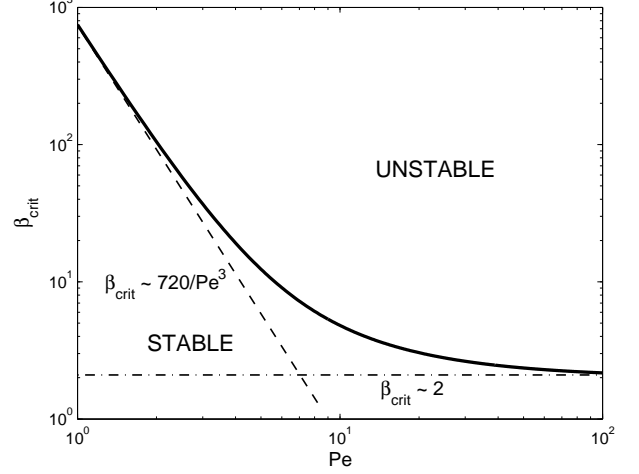


FIG. 2. Critical bacteria concentration  $\beta_{crit}$  as a function of the Peclet number (solid line). The dashed lines are the asymptotic results:  $\beta_{crit} \sim 720/Pe^3$  for  $Pe \ll 1$  and  $\beta_{crit} \sim 2$  for  $Pe \gg 1$ .

where  $\alpha$  is a function of Peclet number given by

$$\alpha = \frac{1}{2Pe} + \left\{ \frac{\exp(-Pe)(1 + Pe) - 1}{Pe^2[1 - \exp(-Pe)]} \right\} - 3 \left\{ \frac{Pe[1 + \exp(-Pe)] + 2[\exp(-Pe) - 1]}{Pe^2[1 - \exp(-Pe)]} \right\}^2 \quad (14)$$

Sinusoidal gap-averaged number density perturbations evolve according to  $\langle n' \rangle = \exp(i2\pi x + \sigma t)$  where the growth rate  $\sigma = (2\pi)^2(Pe\alpha\beta - 1)$ . Since both  $\alpha$  and  $Pe$  are positive, instability occurs if  $\beta$  exceeds the critical value  $\beta_{crit} = (\alpha Pe)^{-1}$ . A suspension of pushers such as *E. Coli* or *B. Subtilis* for which  $\beta$  is positive, is unstable to number density variations in the  $x$  direction above a critical concentration while puller suspensions having negative  $\beta$  will be unconditionally stable. Fig. 2 shows that the critical bacteria concentration  $\beta_{crit}$  decreases with increasing Peclet number reaching an asymptote of 2 at high Peclet number.

The mechanism of the instability is illustrated in Fig. 1. The chemical gradient leads to a base state number density profile  $n_0(z)$  that is an exponentially decreasing function of  $z$  and causes a net alignment of the cells in the  $-z$  direction. The disturbance flow of each cell draws fluid in from the sides and pushes it out at the front and back. A sinusoidal perturbation in the gap-averaged number density,  $\langle n' \rangle$ , leads to a number density field,  $n'$  with alternate peaks and valleys (brighter and darker regions respectively in Fig. 1) at  $z = 0$  owing to the competition of chemotaxis and diffusion in controlling the local  $z$ -number-density profile. Being pushers, the excess bacteria at peaks draw fluid inward at small  $z$  while the fluid returns toward valleys at larger values of  $z$ . This fluid

velocity field acting on the base state number density field leads to a net gap-averaged convective flux  $\langle u'_x n_0 \rangle$  toward the region of high  $\langle n' \rangle$ , thereby reinforcing the number density perturbation. In the sub-critical regime,  $x$ -diffusion of the bacteria attenuates the concentration perturbations and stabilizes the suspension. Since the hydrodynamic disturbance of a puller is exactly opposite to that of a pusher, a suspension of pullers is always stable. Since  $\sigma$  is purely real, the instability is stationary at least in the long-wavelength limit and the streamline pattern resembles convection cells. A result of the lubrication approximation is that the dimensional growth rate increases quadratically in the wavenumber  $2\pi/\lambda$ . However, at sufficiently large wavenumbers one expects diffusion to stabilize the suspension implying that a mode of maximum growth rate should exist. The wavelength of the most unstable mode can come only from a finite wavelength analysis with  $\lambda \sim H$  or smaller. This instability might be expected to lead to the formation of periodic clusters of bacteria within the channel or film along  $x$  axis with a length scale corresponding to the most unstable mode.

Sokolov *et al.* [6] observed three-dimensional convective motions in films of aerobic bacteria with half-thickness greater than  $100 \mu\text{m}$ . We refer to the half-film thickness here since the gradient of the attractant oxygen acts from the mid-plane to the interface when the film is thick enough so that the bacteria consume oxygen before it diffuses to the mid-plane. Although this experiment involves a thin film with gas-liquid interfaces, Marangoni stresses usually lead to a nearly inextensible nature of such interfaces making the no slip boundary condition appropriate. The bacterial concentration in Sokolov *et al.*'s [6] experiments is  $\langle n_0 \rangle \approx 2 \times 10^{10}$  per milliliter. Using  $L = 12 \mu\text{m}$  and  $H = 100 \mu\text{m}$ , the scaled bacteria concentration is  $\beta = 60$ . It is clear from Fig. 2 that this value exceeds  $\beta_{crit}$  if  $Pe \geq 2.50$ . This corresponds to  $U_0/U \geq 0.17$  for a typical bacterial swimming speed of  $20 \mu\text{m/s}$  and a typical tumbling frequency of  $1 \text{ s}^{-1}$  [10]. This value of  $U_0/U$  is sufficiently small to make the small  $\zeta$  analysis accurate. The chemotactic velocity is not known in Sokolov *et al.*'s [6] experiments. Nevertheless, the above analysis suggests a moderate amount of chemotaxis can drive the instability. The mode of instability predicted here is consistent with Sokolov *et al.*'s [6] observations of convection across the film half-thickness and plumes of bacteria concentration.

The present instability mechanism differs from previous for active-stress instabilities [1–4, 12]. Since the active bacterial stress depends on both the number density and orientation distribution of the bacteria, instability can arise from the coupling between either the number density field or the orientation field and the fluid flow. Previous stability analyses have focused on coupling of fluid shearing motion and swimmer alignment in

unbounded homogeneous suspensions of isotropic [3, 4] or aligned swimmers with [12] or without chemotaxis [2, 3]. In these cases it is found that the unstable modes do not involve bacteria number density variations at leading order in the long wavelength limit. A fluid velocity perturbation to an isotropic (or nearly isotropic) suspension tends to align the bacteria to the extensional axis of the fluid velocity field. The hydrodynamic disturbance of a pusher then enhances the original velocity perturbation resulting in an orientation-shearing instability. It is possible that this instability accounts for the two-dimensional motion with no apparent bacteria concentration variation observed by Sokolov *et al.* [6] at small film thickness. The instability mechanism described in the present Letter relies on a base state with a stratified number density profile. Fluid motion can then lead to a three-dimensional number density profile and concomitant active stress profile that enhances the number density variation in the case of pushers. In Sokolov *et al.*'s [6] experiments, such an instability is to be expected when the film is thick enough to allow oxygen and cell gradients to develop across the film half-thickness. A more definitive experimental test of the theory proposed in this Letter could be obtained using an experimental cell [8] that allows the cells to experience a controlled linear gradient of a chemo-attractant that is not consumed by the cells.

This work is supported by NSF grant CBET-0730579.

- 
- [1] D. L. Koch and G. Subramanian, *Annu. Rev. Fluid Mech.* **43**, 637 (2011).
  - [2] R. A. Simha and S. Ramaswamy, *Phys. Rev. Lett.* **89**, 058101 (2002).
  - [3] D. Saintillan and M. J. Shelley, *Phys. Rev. Lett.* **100**, 178103 (2008); *Phys. Fluids* **20**, 123304 (2008).
  - [4] G. Subramanian and D. L. Koch, *J. Fluid Mech.* **632**, 359 (2009).
  - [5] M. J. Kim and K. S. Breuer, *Anal. Chem.* **79**, 955 (2007).
  - [6] A. Sokolov, R. E. Goldstein, F. I. Feldchtein, and I. S. Aranson, *Phys. Rev. E* **80**, 031903 (2009).
  - [7] T. J. Pedley and J. O. Kessler, *Annu. Rev. Fluid Mech.* **24**, 313 (1992); A. J. Hillesdon and T. J. Pedley, *J. Fluid Mech.* **324**, 223 (1996).
  - [8] S. Cheng, S. Heilman, M. Wasserman, S. Archer, M. Shuler, and M. Wu, *Lab Chip* **7**, 763 (2007).
  - [9] R. Mesibov and J. Adler, *J. Bacteriol.* **112**, 315 (1972).
  - [10] H. C. Berg, *E. coli in Motion* (Springer Verlag, 2003).
  - [11] D. A. Brown and H. C. Berg, *Proc. Natl. Acad. Sci. U.S.A.* **71**, 1388 (1974); K. C. Chen, R. M. Ford, and P. T. Cummings, *J. Math. Biol.* **47**, 518 (2003).
  - [12] G. Subramanian, D. L. Koch, and S. R. Fitzgibbon, *Phys. Fluids* **23**, 041901 (2011).
  - [13] R. R. Vuppula, M. S. Tirumkudulu, and K. V. Venkatesh, *Phys. Biol.* **7**, 026007 (2010).
  - [14] E. Keller and L. Segel, *J. Theor. Biol.* **30**, 225 (1971); R. N. Bearon, *Phys. Fluids* **15**, 1552 (2003).